Multi-actuator adaptive lens in astronomy: in lab test results

Magrin, D., Favazza, P., Bonora, S., Quintavalla, M., Bergomi, M., et al.

D. Magrin, P. Favazza, S. Bonora, M. Quintavalla, M. Bergomi, R. Ragazzoni, "Multi-actuator adaptive lens in astronomy: in lab test results," Proc. SPIE 10703, Adaptive Optics Systems VI, 1070374 (13 July 2018); doi: 10.1117/12.2313382

SPIE.

Event: SPIE Astronomical Telescopes + Instrumentation, 2018, Austin, Texas, United States

Multi-Actuator Adaptive Lens in Astronomy: in lab test results

D. Magrin[a,b], P. Favazza [d], S. Bonora[c], M. Quintavalla[c], M. Bergomi[a,b], R. Ragazzoni[a,b]

[a]INAF - Osservatorio Astronomico di Padova, Vicolo dell'Osservatorio 5, 35122 Padova, Italy
[b]ADONI –Laboratorio Nazionale di Ottica Adattiva
[c]CNR-IFN – Istituto di Fotonica e Nanotecnologie, via Trasea 7, 35131 Padova, Italy
[d]Dipartimento di Fisica ed Astronomia -Università degli Studi di Padova, Vicolo dell'Osservatorio 3, 35122 Padova, Italy

ABSTRACT

Multi-actuator Adaptive Lenses have been recently utilized for the implementation of Adaptive Optics in different scientific fields such as microscopy, in vivo ophthalmic imaging applications or high power laser beam shaping.
A multi-actuator adaptive lens is composed by two thin glass plates bonded to two piezoelectric rings with 18 actuators. The space between the two glass plates is filled with a transparent liquid and the actuation of the lens allows a wavefront modulation up to the 4th order of Zernike polynomials with a relatively fast time response (frequency up to 200Hz). These features allow using the adaptive lens in closed loop with wavefront sensor as if it were a deformable mirror. Despite the adaptive lenses performances do not allow their use in extreme astronomical instrumentation as substitutes for deformable mirrors, they are the ideal device for the correction of the non-common path aberrations in order to maximize the performances of the pyramid wavefront sensor.
In this paper, we present the laboratory results of a characterization campaign of an adaptive lens prototype manufactured for astronomical applications and its use to correct non-common path aberrations to enhance pyramid wavefront sensor sensitivity.

Keywords: Adaptive lens, NCP aberrations, Pyramid WFS, SCAO, XAO

1. INTRODUCTION

The Adaptive Lens (AL) is a refractive deformable optical element able to change its shape thanks to piezoelectric actuators placed on its external diameter. The relatively small number of actuators and the response frequency exclude the possibility to substitute the Deformable Mirror (DM) with an AL in their typical application on an Adaptive Optics (AO) system. However, AL has already demonstrated its potentiality as wavefront corrector in different scientific fields such as in microscopy, in vivo ophthalmic imaging applications or in high power laser beam shaping. Thanks to the AL compactness and to the possibility to place it in a collimated beam of a pre-existing optical system without the needs to add other optics or changing the optical path, its use is appealing also in the astronomical fields. In particular, we aim to correct the non-common path aberrations (NCPA) in a Single Conjugate Adaptive Optics (SCAO) system working in closed loop with a pyramid wavefront sensor and a DM.

2. NCPA CORRECTION WITH AN ADAPTIVE LENS

The Pyramid Wavefront Sensors (P-WFS) was proposed for the first time in 1996 [1]. Within few years, its potentiality was demonstrated on sky at the Telescopio Nazionale Galileo (TNG) [2, 3] in the Canary Islands. Nowadays, P-WFS is largely preferred to the, previously more popular, Shack-Hartmann wavefront sensor (SH-WFS) in several AO system [4, 5, 6, 7]. One of the most important milestones of the P-WFS success is probably represented by the outstanding results [8] obtained by the First Light Adaptive Optics (FLAO) system at Large Binocular Telescope (LBT) in 2010.

The intrinsic advantages of the P-WFS with respect to the SH-WFS lays on the fact that as the closed loop iterations increase, and the PSF of the reference natural star on the pin of the pyramid becomes smaller, the sensitivity of the P-WFS increases [9, 10]. P-WFS presents also the technical advantage to allow the sampling of the pupil sub-apertures at

Adaptive Optics Systems VI, edited by Laird M. Close, Laura Schreiber, Dirk Schmidt, Proc. of SPIE Vol. 10703, 1070374 · © 2018 SPIE
CCC code: 0277-786X/18/$18 · doi: 10.1117/12.2313382

the detector level, and therefore offers the possibility to sense a different number of modes by simply acting on the detector pixels binning.

On the contrary, it has also been shown that the sensitivity gain of the P-WFS with respect to the SH-WFS can rapidly drop with the quality degradation of the reference star PSF (low Strehl Ratio) on the pin of the pyramid [11]. This difference from the optimal P-WFS working regime can depend on many factors. One of them is represented by the presence of NCPA between the scientific channel and the wavefront sensing channel, which could originate from design mismatching, poor relative alignment but also from gravity and thermal differential effects.

The NCPA correction is typically achieved in a closed loop system by introducing an offset to the signal sent to the deformable mirror corresponding to the wavefront differences between the instrument and the wavefront sensor. In the case of the P-WFS, depending on the severity of the NCPA amplitude, this offset may reduce the overall potential performance of the AO system. In particular, Figure 1 [11] shows the variation of the limiting magnitude gain of the P-WFS with respect to the SH-WFS as a function of the achieved Strehl Ratio (SR) on the pyramid pin for different D/r_0 representing the maximum radial order that can be corrected by the AO system, where D is the entrance pupil diameter of telescope and r_0 the size of the actuator projected on the pupil (here assumed equal to the Fried parameter). The dash line represents the maximum achievable SR value related to the maximum corrected radial order. For a wavefront sensor working in the visible band at an 8-m class telescope D/r_0 it is usually about 40.

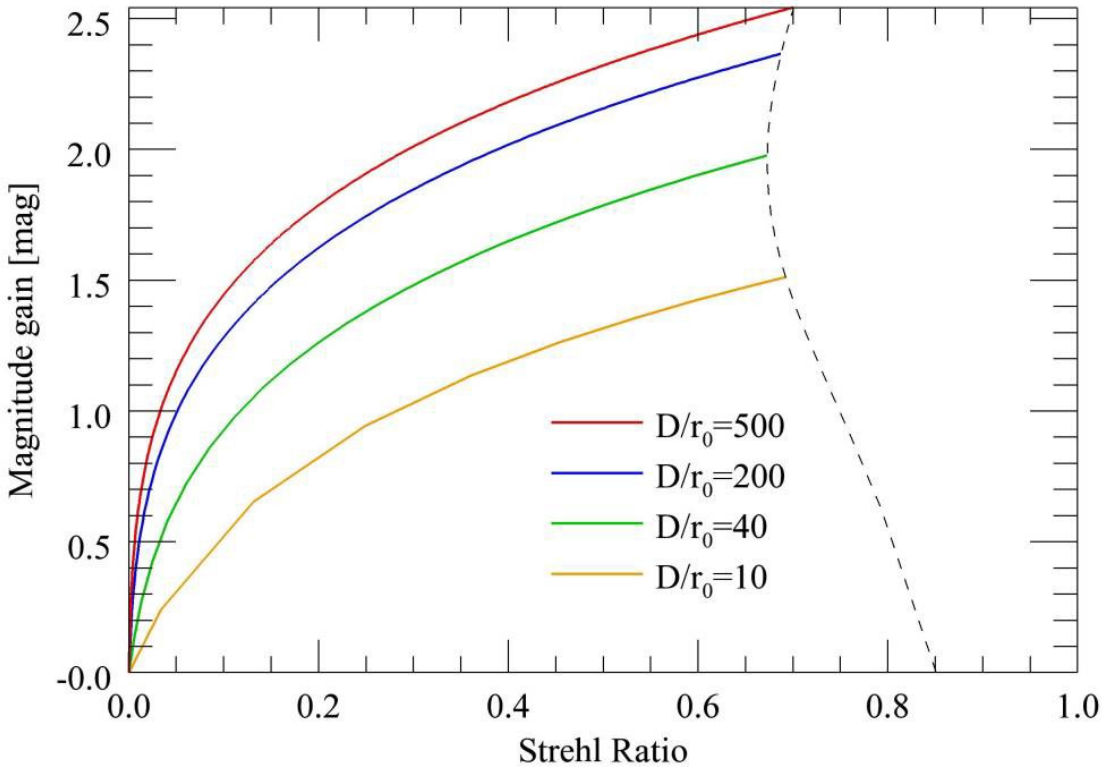

Figure 1. Gain in limiting magnitude of the P-WFS versus SH-WFS as function of the achieved Strehl Ratio (SR) on the pyramid pin for different D/r_0. The dash line represents the limit in the maximum SR that can be obtained for each D/r_0.

In order to give a quantitative idea of the effect, let's assume that in a P-WFS based SCAO system in closed loop the SR reached on the pyramid pin is about 20% (corresponding to about 0.2 RMS wave of aberration) and that 0.1RMS wave of NCPA (compensated by introducing an offset to the signal sent to the DM) are contributing to it. If, in some way, the contribution of the NCPA can be neglected, the SR on the pyramid pin in the case of an 8-m class telescope raises to about 67%, translating in a potential gain in terms of limiting magnitude of about 0.7 magnitude.

Basically, the idea we propose is to insert in the optical path an Adaptive Lens [12] able to mitigate for the low orders NCPA the aberrations reaching the pyramid pin. With reference to Figure 2, the AL applies an opposite wavefront deformation with respect to the signal offset sent to the DM. Usually the NCPA are measured when the system is in closed loop and the P-WFS are in the best regime, by estimating the image quality on the scientific detector of the instrument. Then the DM is piloted in order to increase the performances on the latter detector. In our scheme, the opposite deformation should be given to the AL so that in principle it can allow the full recovery of the pyramid gain even in NCPA correction mode. In this case, the AL is piloted in open loop. For non-static NCPA, the correction can take advantage of pre-calibrated lookup tables in different observing conditions. If the scientific instrument includes an internal wavefront sensing system able to continuously monitor in real time the image quality, it is in principle possible to correct the NCPA on the DM and counter correct the wavefront on the P-WFS by AL in closed loop.

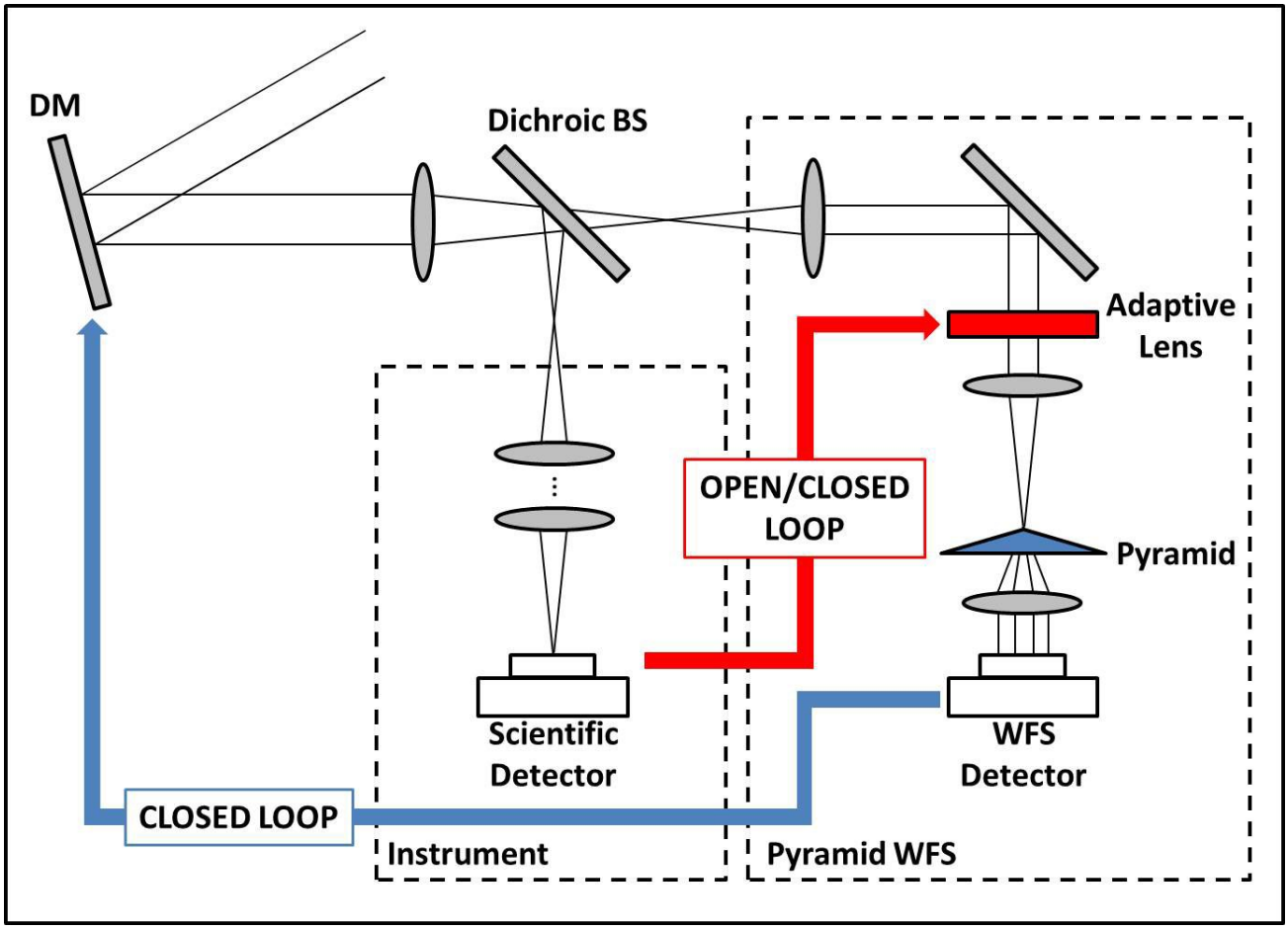

Figure 2. Possible scheme of NCPA correction through Adaptive Lens.

The refractive nature, compactness and the clear aperture sizes of the AL make this device suitable for an easy installation on board of already existing P-WFS systems without the need of complex re-design or insertion of folding mirrors. Typically, NCPA are low-order aberrations and presents a slow evolution with time. The 15 correction modes and the 200Hz frequency, makes the Al suitable for this application.

It has to be underlined that in many already existing AO systems, the NCPA are mostly generated by dichroic plates placed in non-collimated beam to split the light between the wavefront sensor and the science channel. Usually this translates into a certain amount of differential astigmatism between the two paths. It has to be underlined here that, given the actuators distribution along the edge of the AL, the astigmatism is one of the best corrected modes.

3. A REFRACTIVE DEFORMABLE ELEMENT: ADAPTIVE LENS

The AL for astronomical application has been manufactured at prototype level. The manufactured AL is composed by two thin N-BK7 optical windows (150 μm thick) filled with transparent liquid, matching the refractive index of the glass. On the outer perimeter of each window piezoelectric (PZT) ring actuators are glued. Both rings are divided into nine sectors that can be actuated independently. The piezoelectric actuators have an external diameter of 25 mm and an internal one of 10 mm with a thickness of 200 μm. The area inside the ring actuator is the clear aperture of the deformable lens and has a diameter of 10 mm. Because the PZT is rigidly glued to the glass disc, its expansion or contraction means that, in first approximation, the unimorph couple formed by the glass and the PZT deforms the glass window as a paraboloid. The local surface lens shape deformation is proportional to the applied voltage.

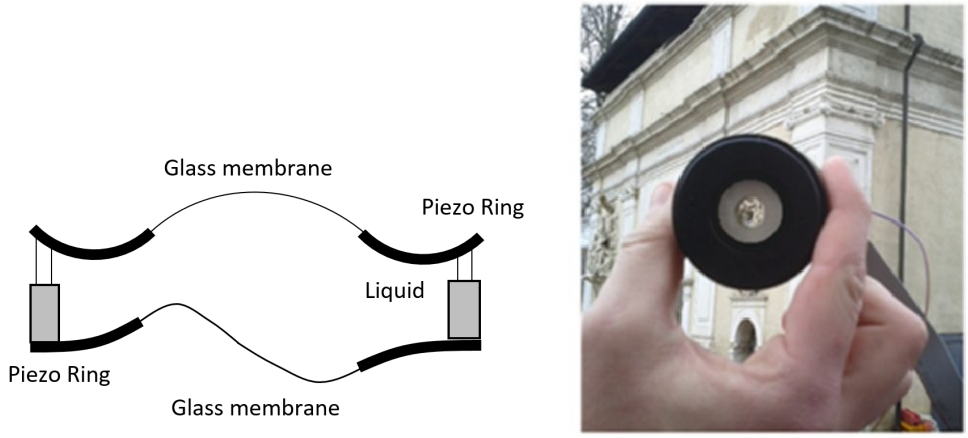

Figure 3. Scheme of the Adaptive Lens. Left side: actuators arrangement. Right side: picture of the AL.

One of the two windows is mounted on a rigid aluminum ring which is necessary to change the boundary condition and to move the maximum (minimum) of the window deformation inside the clear aperture. Therefore, the activation of electrodes in the two windows gives a different lens shape. It has to be underlined that at the moment the windows external surfaces are not AR coated, probably accounting for most of the throughput losses involved in this prototype.

The wavefront of a collimated beam passing through the AL is basically given by the difference of the shape of the two optical windows multiplied by the refractive index of the transparent liquid contained on the lens. The shape of each window is determined by the applied voltages and can be well approximated by the algebraic sum of the deformation induced by each single electrode in both windows. The actuators are controlled using a 18-channel high voltage (+/-125 V) driver. The maximum allowed frequency is about 200 Hz.

4. LABORATORY SETUP

An ad hoc laboratory setup has been assembled in order to start a test campaign on the AL. During this first phase of the test campaign, just the AL has been implemented in the optical setup excluding the use of a DM.

With reference to Figure 4, a 10 mm collimated monochromatic beam passes through an AL. The beam is then separated in two by a beam splitter. The transmitted beam proceeds through the P-WFS arm. This arm includes a Barlow lens with an equivalent focal length of about 1000 mm. On the focal plane it is placed the pin of a pyramid having a vertex angle of 1 degree. The size of the PSF over the pyramid pin is about 60 micron mitigating the manufacturing quality effects of the pin itself. A second lens, having focal length of 100 mm, then collimates the beam and forms the images of the four pupils on a CCD, having diameter of about 1 mm and lateral separation of about 1.25 mm. The reflected beam goes through the SH-WFS arm. In this arm, the beam is de-magnified to a diameter of 3 mm through two properly dimensioned lenses allowing the pupil sampling by a micro-lenses array having format 40×40 and lens pitch equal to 150 micron and focal length 5.139 mm. The sampling in this way is 20 sub-apertures over the pupil diameter. The optical setup has been aligned and fully characterized.

In this setup the AL can be driven in closed loop by both the P-WFS and by SH-WFS. The influence matrixes for both the driven modes have been measured and implemented into a semi-automatic control software.

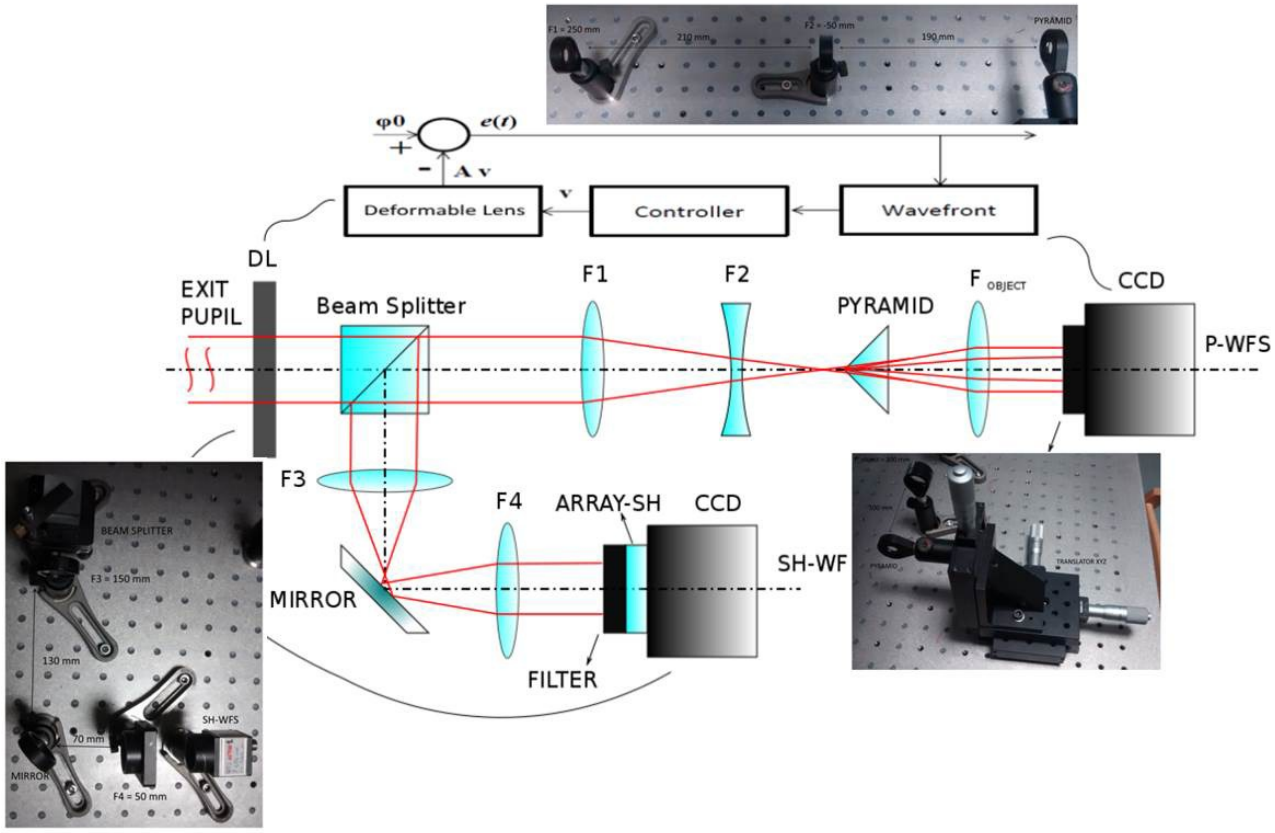

Figure 4. Scheme of the Laboratory setup.

5. MEASUREMENTS RESULTS

We determined the value of the non-common path aberrations on the pyramid arm using a hill climbing optimization method [12]. In this technique, we used the adaptive lens in order to generate a bias aberration while measuring a merit function that we want to minimize. In this case, the merit function was the rms wavefront error on the pyramid wavefront measurement. The bias aberrations were generated as Zernike polynomials (see for more details [13]) from the lower order to the third order. After this procedure the aberration measured by the SH wavefront sensor was about 0.1waves rms (see Figure 5) while the aberration on the pyramid wavefront sensor was reduced down to 0.01 waves rms. The 0.1 waves rms represents the NCPAs between our two arms.

We also investigated the long term stability of the adaptive lens correction. The lens was initially driven in closed loop with the P-WFS, and the the loop was opened maintaining the AL actuators in the same configuration. Figure 6 reports the rms aberration stability over 30 minutes. The measurement reports a variation of about 7% mainly caused by piezoelectric actuators creep effect. As reported in Figure 6 left the main long term aberration variation is caused by defocus and astigmatism. Figure 6 right shows the variation of the measurement on pyramid wavefront sensor. Again this measurement shows that the main varying aberrations are defocus and astigmatism.

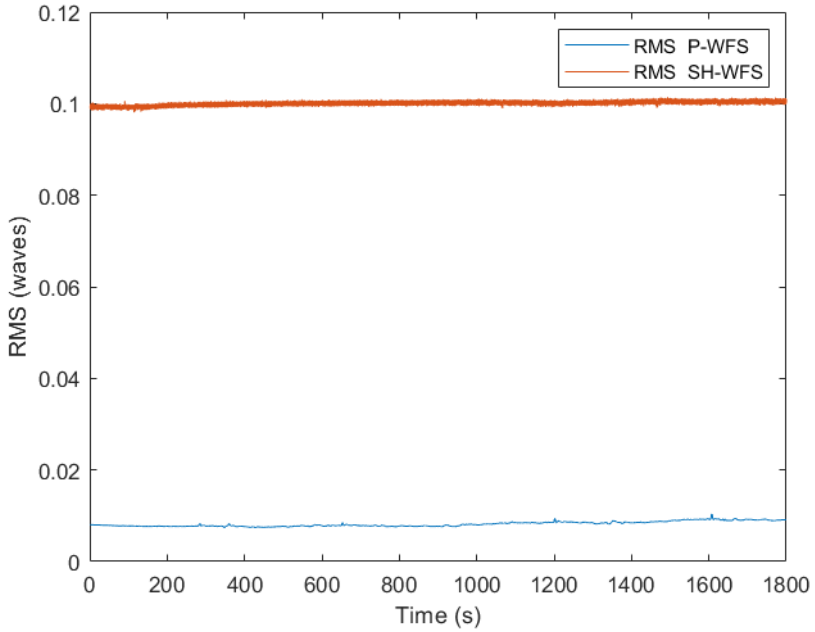

Figure 5. Measurement with the SH of the non-common path aberration.

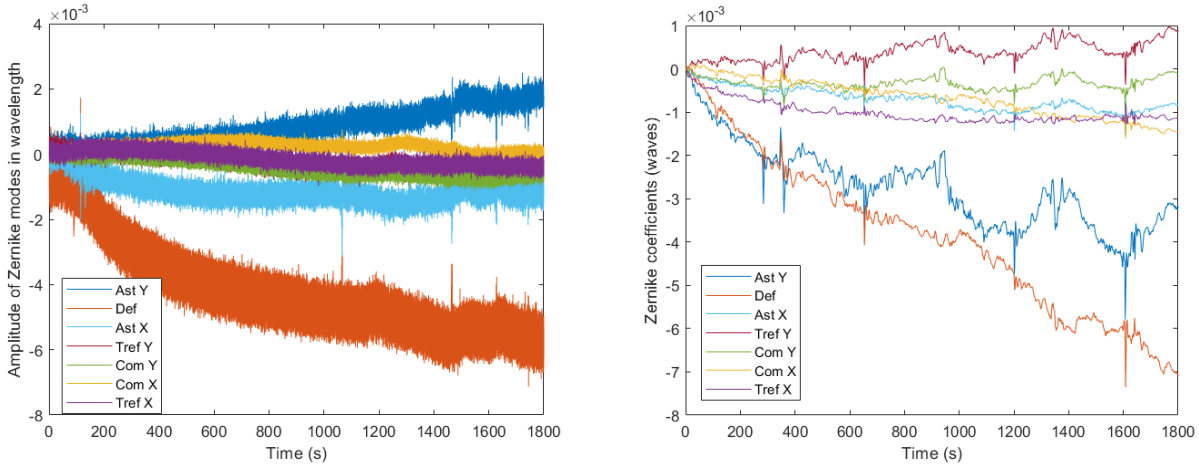

Figure 6. Measurement of the stability of the non-common path aberrations on the Shack Hartmann (left) and on the Pyramid (right) over 1800 seconds. This measurement reports the Zernike NCPA decomposed in Zernike polynomials with the average aberration removed.

6. CONCLUSIONS

During the first part of the AL laboratory characterization, obtained results are promising. The AL capability to correct low order NCPAs of the magnitude order of 0.1 wave rms has been demonstrated to be feasible. The actuators creep effect over 30 minutes with the AL in open loop seems acceptable at this working level. In the next phase, we will install on the setup a DM in order to reproduce a SCAO system, characterizing the behaviour of the AL and its capability to correct the NCPA with the pyramid in closed loop with the DM.

REFERENCES

[1] Ragazzoni, R. "Pupil plane wavefront sensing with an oscillating prism", J. Modern Opt. 43, 289-293 (1996).

[2] Ragazzoni, R.; Baruffolo, A.; Farinato, J.; Ghedina, A.; Marchetti, E.; Niero, T. "Toward Adopt a TNG First Light", Astronomy with adaptive optics : present results and future programs, Proceedings of an ESO/OSA topical meeting, 651-657 (1998)

[3] Ragazzoni, R., Baruffolo, A., Farinato, J., Ghedina, A., Marchetti, E., Esposito, S., Fini, L., Ranfagni, P., Bortoletto, F., D'Alessandro, M., Ghigo, M., Crimi, G. "Final commissioning phase of the AdOpt@TNG module", Proc. SPIE, 57-62 (2000)

[4] Morzinsky, K. M.; Close, L. M.; Males, J.; Kopon, D.; Hinz, P. M.; Esposito, S.; Riccardi, A.; Puglisi, A.; Pinna, E.; Briguglio, R.; Xompero, M.; Quirós-Pacheco, F.; Bailey, V.; Follette, K. B.; Rodigas, T. J.; Wu, Y.-L.; Arcidiacono, C.; Argomedo, J.; Busoni, L.; Hare, T.; Umamoto, A.; Weinberger, A. "MagAO: Status and on-sky performance of the Magellan adaptive optics system", Proc. SPIE 9148, (2014).

[5] Jovanovic, N; Martinache, F.; Guyon, O.; Clergeon, C.; Singh, G.; Kudo, T.; Garrel, V.; Newman, K.; Doughty, D.; Lozi, J.; Males, J.; Minowa, Y.; Hayano, Y.; Takato, N.; Morino, J.; Kuhn, J.; Serabyn, E.; Norris, B.; Tuthill, P.; Schworer, G.; Stewart, P.; Close, L.; Huby, E.; Perrin, G.; Lacour, S.; Gauchet, L.; Vievard, S.; Murakami, N.; Oshiyama, F.; Baba, N.; Matsuo, T.; Nishikawa, J.; Tamura, M.; Lai, O.; Marchis, F.; Duchene, G.; Kotani, T.; Woillez, J "The Subaru Coronagraphic Extreme Adaptive Optics System: Enabling High-Constrast Imaging on Solar-System Scales", PASP 127, 890-910 (2015).

[6] Esposito, S.; Riccardi, A.; Fini, L.; Puglisi, A. T.; Pinna, E.; X., Marco; Briguglio, R.; Quirós-Pacheco, F.; Stefanini, P.; Guerra, J. C.; Busoni, L.; Tozzi, A.; Pieralli, F.; Agapito, G.; Brusa-Zappellini, G.; Demers, R.; Brynnel, J.; Arcidiacono, C.; Salinari, P. "First light AO (FLAO) system for LBT: final integration, acceptance test in Europe, and preliminary on-sky commissioning results", Proc. SPIE v. 7736 (2010)

[7] Riccardi, A.; Antichi, J.; Quirós-Pacheco, F.; Esposito, S.; Carbonaro, L.; Agapito, G.; Biliotti, V.; Briguglio, R.; Di Rico, G.; Dolci, M.; Ferruzzi, D.; Pinna, E.; Puglisi, A.; Xompero, M.; Marchetti, E.; Fedrigo, E.; Le Louarn, M.; Conzelmann, R.; Delabre, B.; Amico, P.; Hubin, N. "The NGS Pyramid wavefront sensor for ERIS", Proc. SPIE, v. 9148, (2014)

[8] Esposito, S.; Riccardi, A.; Pinna, E.; Puglisi, A.; Quirós-Pacheco, F.; Arcidiacono, C.; Xompero, M.; Briguglio, R.; Agapito, G.; Busoni, L.; Fini, L.; Argomedo, J.; Gherardi, A.; Brusa, G.; Miller, D.; Guerra, J. C.; Stefanini, P.; Salinari, P. "Large Binocular Telescope Adaptive Optics System: new achievements and perspectives in adaptive optics", Proc.SPIE, v. 8149, (2011)

[9] Ragazzoni, R.; Farinato, J "Sensitivity of a pyramidic Wave Front sensor in closed loop Adaptive Optics", A&A, v. 350, 23-26 (1999)

[10] Vérinaud, C. "On the nature of the measurements provided by a pyramid wave-front sensor", Optics Communications 233, 27-38 (2004).

[11] Viotto, V.; Ragazzoni, R.; Bergomi, M.; Magrin, D.; Farinato, J. "Expected gain in the pyramid wavefront sensor with limited Strehl ratio", Astronomy & Astrophysics, Volume 593, (2016)

[12] Stefano Bonora, Yifan Jian, Pengfei Zhang, Azhar Zam, Edward N. Pugh, Robert J. Zawadzki, and Marinko V. Sarunic, "Wavefront correction and high-resolution in vivo OCT imaging with an objective integrated multi-actuator adaptive lens," Opt. Express 23, 21931-21941 (2015)

[13] M. J. Booth, Wavefront sensorless adaptive optics for large aberrations, Opt. Lett. 32, 5 (2007).